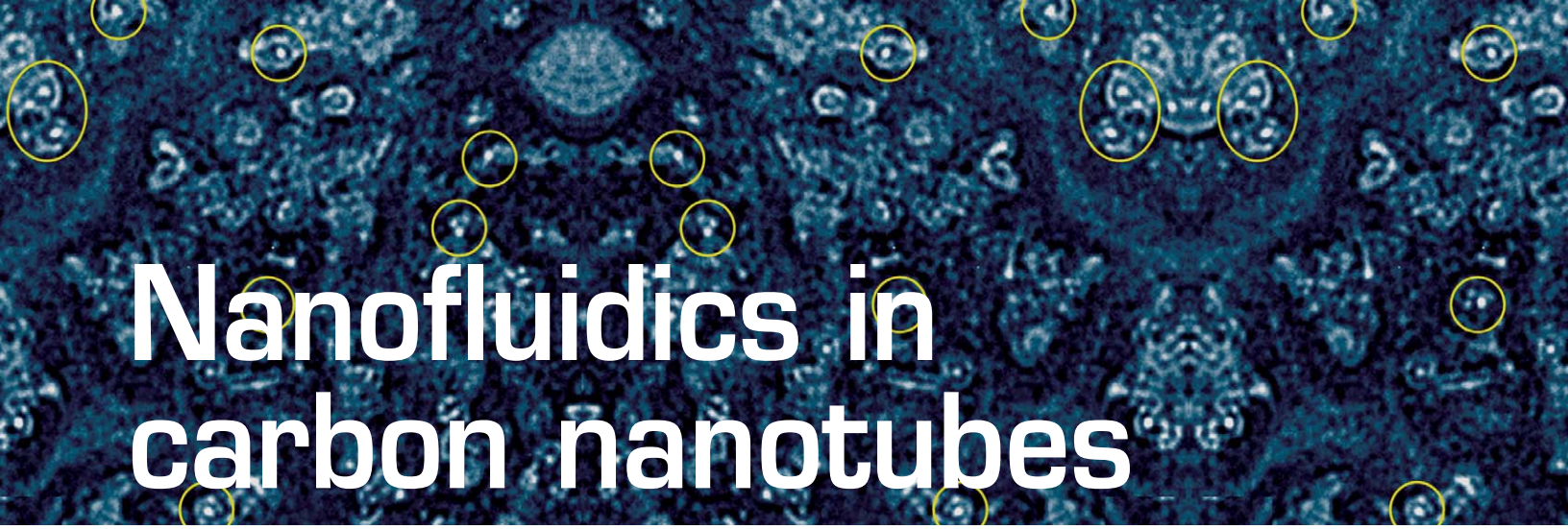

Nanofluidics in carbon nanotubes

Extremely high aspect ratios, molecularly smooth hydrophobic graphitic walls, and nanoscale inner diameters of carbon nanotubes give rise to the unique phenomenon of ultra-efficient transport of water and gas through these ultra-narrow molecular pipes. Water and gas molecules move through nanotube pores orders of magnitude faster than through other pores of comparable size. The proposed water transport mechanism has a distinct similarity to the transport mechanisms of biological ion channels. Molecular dynamics simulations and experimental measurements of water transport underscore the importance of nanotube structure in enabling ultra-efficient transport through the pore.

Aleksandr Noy[a]*, Hyung Gyu Park[a,b], Francesco Fornasiero[a], Jason K. Holt[a], Costas P. Grigoropoulos[b], and Olgica Bakajin[a†]

[a]Molecular Biophysics and Functional Nanostructures Group, Chemistry, Materials and Life Sciences Directorate, Lawrence Livermore National Laboratory, Livermore, CA 94550, USA

[b]Department of Mechanical Engineering, University of California at Berkeley, Berkeley, CA 94720-1740, USA

*E-mail: *noy1@llnl.gov, †bakajin1@llnl.gov*

A rare combination of transport efficiency and selectivity makes carbon nanotube (CNT) membranes a promising technology for the next generation of water desalination, water purification, nanofiltration, and gas separation applications. CNT membranes are also a versatile and truly powerful nanoscale platform for fundamental studies of nanofluidics.

What is nanofluidics?

Limits of continuum hydrodynamics

Classical continuum hydrodynamics governed by Navier–Stokes equations successfully describes the dynamic behavior of water (fluid flow) on the macroscopic scale. In the continuum fluid hypothesis, both state and dynamic variables such as density, temperature, and velocity vary in a continuous and differentiable fashion with respect to the position in the fluid and to time. Thus the continuum theory formalism is independent of the nature of the molecular structure and configuration[1]. Advances in nanoscience, which have relentlessly pushed the dimensions of synthetic objects closer to the molecular scale, pose an important fundamental question: does the continuum-based description of fluid flow still work in a situation where the reduction in the system size causes those variables to vary appreciably over the molecular length and relaxation time scales? To answer this question, we can estimate the smallest size of water droplet that still can be treated as a continuum object. Simple reasoning tells us that to obtain less than 1% statistical fluctuation (or 1% statistical resolution) of a physical property we need ~10 000 particles. A sphere containing 10 000 equidistant water molecules has a diameter of ~27 molecules, or ~6.5 nm. Researchers have also tried to use nonequilibrium

ISSN:1748 0132 © Elsevier Ltd 2007

molecular dynamics (MD) to pin down the length scale at which the continuum model starts to break down. For example, Travis *et al.*[2] have determined that velocity profiles of a simple fluid composed of nonstructured molecules starts to approach Navier–Stokes theory predictions when the channel width approaches ten molecular diameters. Simulations of electro-osmotic flow by Qiao and Aluru[3] indicate that continuum flow theory can be used to predict bulk fluid flow in channels as small as 2.22 nm but only if the viscosity variation near the channel wall is taken into account. Huang *et al.*[4] have simulated 2.2 nm diameter pores and shown that as solid-liquid interactions are varied away from neutral-like interactions, the Navier–Stokes equations start to break down. Even though a consensus on the exact scale where continuum models break down has not emerged yet, it is clear that flow through CNTs with lateral dimensions of less than 2 nm would fall in the domain of the nascent field of noncontinuum fluidics, or *nanofluidics*.

Basic structure and properties of CNTs

By now, the CNT has firmly established itself as the iconic molecule of nanoscience[5]. Despite having a very simple chemical composition and structure, a CNT is capable of displaying an astonishing variety of unique properties. A CNT is simply a nanosized rolled-up graphene sheet forming a perfect seamless cylinder (Fig. 1) capped at the ends by fullerene caps. It is common to characterize the structure of the nanotube by its rolled-up vector (*n,m*), called chirality or helicity, which defines the position of the matched carbon rings during the roll-up of the graphene sheet[6]. Significantly, this roll-up vector fully defines the nanotube morphology, its diameter, and its electronic properties. For example, an (*n,m*) CNT has an inner diameter, d_{in}, of[6]:

$$d_{in} = (a/\pi)\sqrt{(n^2 + m^2 + nm)} - 2r_c$$

where a is the lattice parameter of graphene (2.5 Å) and r_c is the van der Waals radius of the carbon atom (1.7 Å).

A CNT can have one (as in case of a single-walled CNT or SWNT), or several concentric graphitic shells (as in case of multiwalled nanotubes or MWNTs). One of the most remarkable properties of this structure, which makes it attractive for transport applications, is its unique combination of extremely high aspect ratio with small dimensions: a nanotube can reach up to several millimeters in length, yet retain a diameter of only a few nanometers. The second important property of CNTs critical for transport applications is the remarkable atomic scale smoothness and chemical inertness of the graphitic walls.

Several methods of CNT production currently exist. In the lab, catalytic chemical vapor deposition (CVD) is preferred over other methods such as arc discharge and laser ablation because it produces higher quality CNTs. CVD reactors can produce individual isolated nanotubes, as well as densely packed vertically-aligned arrays (Fig. 1c). Unfortunately, the ultimate goal of CNT synthesis – producing a uniform population of nanotubes with a given chirality – still remains elusive. Several studies indicate that the size of the catalyst particle during growth determines the size of the CNT to less than 10%[7]; yet the efforts to control the size of CNTs with greater precision have been largely unsuccessful. Thus, synthesizing a vertically aligned CNT array with a narrow size distribution still remains a difficult endeavor requiring considerable process development and optimization[7–9]. A description of the details of CNT synthesis goes beyond the scope of this article, but can be found in other recent reviews[10–12].

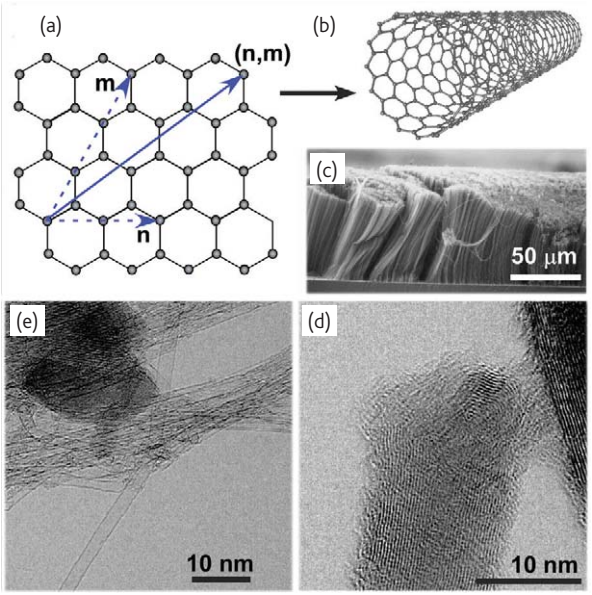

Fig. 1 Structure and morphology of CNTs. (a) Schematic of a graphene sheet and a CNT roll-up vector. The roll-up vector (n,m) is perpendicular to the axis of the CNT. (b) A three-dimensional model of a SWNT. (c) A scanning electron microscope (SEM) image of a vertically aligned array of MWNTs grown on a Si substrate. (SEM image courtesy of M. Stadermann, O. Bakajin and A. Noy, LLNL.) Transmission electron microscopy (TEM) images of (d) MWNTs and (e) SWNTs. (TEM images courtesy of J. Plitzko and A. Noy, LLNL.)

Simulations of water and gas in CNTs

Water inside CNTs

The task of observing and understanding fluid and gas flows in CNT pores raises a set of unique fundamental questions[13]. First, it is surprising that hydrophilic liquids, especially water, enter and fill very narrow and hydrophobic CNTs. If water does enter CNTs, what influence does extreme confinement have on the water structure and properties? It is important to evaluate how these changes in structure influence the rates, efficiency, and selectivity of the transport of liquids and gases through CNTs. As is often the case, MD simulations have provided some of the first answers to these questions. Hummer *et al.*[14] have used MD simulations to observe (Figs. 2a,b) the filling of a (6,6) CNT (0.81 nm in diameter and 1.34 nm in length) with water molecules. Surprisingly, they find that water fills the empty cavity of a CNT within a few tens of picoseconds and the filled state continues over the entire simulation time (66 ns). More importantly, the water molecules confined in such a small space form a single-file

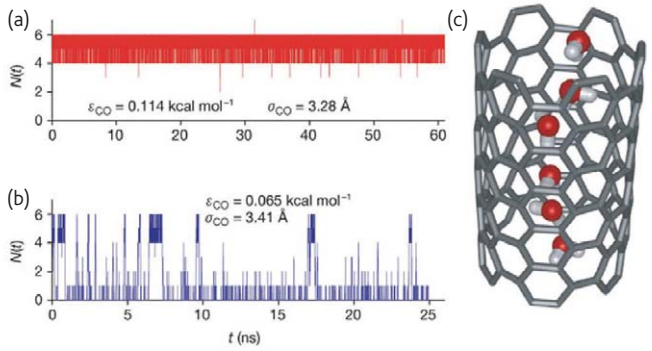

Fig. 2 MD simulations of water and proton transport in CNTs. Number N of water molecules inside an 8.1 Å diameter nanotube as a function of time for sp^2 carbon parameters (a) and reduced carbon–water attractions (b). (c) Structure of the hydrogen-bonded water chain inside a CNT. (Reproduced with permission from[14]. © 2001 Nature Publishing Group.)

configuration that is unseen in the bulk water. Several experimental studies also provide some evidence of water filling of CNTs[15–18]. Further analysis of the simulation results of Hummer *et al.* shows that water molecules inside and outside a nanotube are in thermodynamic equilibrium. This observation illustrates one of the more important and counterintuitive phenomena associated with nanofluidic systems: nanoscale confinement leads to a narrowing of the interaction energy distribution, which lowers the chemical potential[14]. In other words, confining a liquid inside a nanotube channel actually lowers its free energy! Further simulations by the same group have shown that the filling equilibrium is very sensitive to water-nanotube interaction parameters: a 40% reduction in the carbon-water interaction potential results in the emptying of the CNT cavity, while a 25% reduction results in a fluctuation between filled and empty states (bi-stable states)[14,19]. This sharp transition between the two states has been observed for other hydrophobic nanopores as well[20–23]. MD simulations have also studied the dependence of CNT hydration on other properties of CNTs such as nanotube wall flexibility[24], charge[25,26], chirality[26,27], length[19], and diameter[25,28,29].

CNTs as biological channel analogs

MD simulations show that a defining feature of water structure in CNTs is the formation of hydrogen-bonded 'water wires' (Fig. 2c) oriented along the nanotube axis[13,14,30]. Such one-dimensional hydrogen-bonded structures are highly reminiscent of the water wires observed in biological channels specializing in water transport, such as aquaporins[31]. In fact, the similarity between aquaporin and CNT channels goes further. Similar to the hydrophobic interior of CNTs, the inner cavity of the aquaporins is lined with hydrophobic residues that facilitate the formation of the one-dimensional hydrogen-bonded water chains[31,32]. Weak interactions of water molecules with the hydrophobic walls combine with the smooth nature of the walls to enable nearly frictionless transport of water. Kalra *et al.*[30] have shown that water moves very rapidly through a nanotube channel under osmotic pressure. They observe that friction at the channel walls in the system is so low that water transport is no longer governed by the Hagen–Poiseuille flow, but instead depends mainly on events at the nanotube entrance and exit. The calculated rates of water transport approach 5.8 water molecules per nanosecond per nanotube. The rates are comparable to water transport rates in aquaporins[33]. Other MD simulations have also observed fast water transport through CNTs[34–36].

One-dimensional water wires also play an important role in proton transport via the Grotthus mechanism in biological structures such as bacteriorhodopsins and cytochromes[37–39]. MD simulations indicate that CNT channels should also facilitate proton transport along the nanotube axis[40]. In these simulations, the calculated proton mobility exceeds proton mobility in bulk water by a factor of 40.

Sorin and Pande[41] have used CNTs to probe the role water plays in the stability of confined proteins. In their simulations, they have observed that the protein helix stability is low for the narrowest CNT and increases monotonically with nanotube diameter. This behavior contradicts classic polymer theory that predicts that peptide helix stability should decrease in this situation. They hypothesize that the main effect of confinement in this system is related to changes in the solvent entropy, which in turn alters the free energy cost of protein-water hydrogen-bond formation and the relative stability of the peptide helix. They conclude that solvent entropy confinement in ultra-narrow channels could affect the rules of protein stability.

MD simulations of gas transport in CNTs

MD simulations also provide an indication that the intrinsic smoothness of the graphene wall of CNTs is a defining feature for the gas phase transport in these channels. Sholl and colleagues have shown that gas flux in CNTs reaches a value almost three orders of magnitude higher than in zeolites with equivalently sized pores (Fig. 3a)[42]. In these simulations, transport diffusivities of light gases such as hydrogen and methane reach almost the same level as that of the bulk gas diffusivity ($O(10^{-1})$ cm^2/s). Depending on the nanotube size, the diffusivity is as large as 10 cm^2/s for hydrogen. In a follow-up set of simulations, the

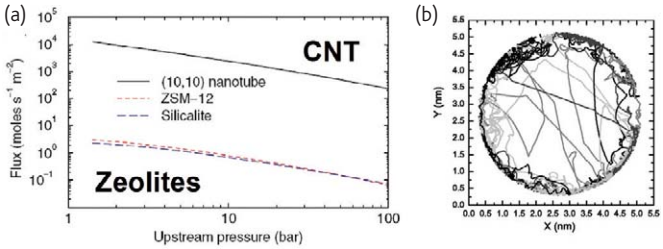

Fig. 3 MD simulations of gas transport through CNTs. (a) Comparison of the predicted methane flux through a 10-μm-thick CNT and other nanoporous materials. (Reprinted with permission from[42]. © 2002 American Physical Society.) (b) Calculated trajectories of CO_2 molecules in a (40,40) CNT at 298 K and a pressure of 1 bar. (Reproduced with permission from[43]. © 2006 American Institute of Physics.)

same group presents a more detailed picture of gas molecule behavior inside a SWNT pore by displaying a density profile and molecular trajectories (Fig. 3b)[43]. The picture of gas transport through CNTs that has emerged from these simulations centers on the predominantly specular nature of the molecule-wall collisions inside CNTs. As a result, a CNT is remarkably effective in allowing gas transport since most of the gas molecules travel along the tube in an almost billiard-ball-like manner[42–45]. Sokhan, Quirke, and others[46–48] have performed a series of MD simulations and reached a similar conclusion to Sholl and coworkers. They simulated both an atomic network of carbons and a smooth imaginary surface with a given slip boundary condition. Maxwell's coefficient or tangential momentum accommodation coefficient (TMAC) determined by the simulation are of the order of 10^{-3} (these values indicate that statistically only 0.1% of gas molecules in the nanotube are thermalized by the wall and randomize their reflection velocities). At the same time, Fig. 3b indicates that some of the gas molecules adsorb on the nanotube walls. Therefore, such behavior could give rise to the alternative mechanism of transport based on two-dimensional surface diffusion[43].

Testing platforms: fabrication of CNT membranes

Testing these seemingly exotic predictions of fast transport through CNTs, which have emerged from MD simulations, has required the fabrication of a robust test platform. Observations of molecular transport through a single nanotube would be a crowning achievement, and Sun and Crooks[49] have made some efforts in that direction. However, practical considerations dictate that experimental efforts focus on a geometry that would allow observation of transport through multiple nanotube pores, such as a *CNT membrane* geometry. These membranes typically consist of an aligned array of CNTs encapsulated by a filler (matrix) material, with the nanotube ends open at the top and bottom. While there are many ways to produce such a structure, (a notable early result by Martin and coworkers was based on fabrication of amorphous CNTs within porous alumina membrane template[50]), the most fruitful approach to date involves growing an aligned array of CNTs, followed by infiltration of a matrix material in between the CNTs (Fig. 4a). The extremely high aspect ratio of the gaps between the nanotubes in the array (length/diameter on order of 1000 or larger) presents a fabrication challenge. Fortunately, researchers have developed successful strategies to overcome this issue.

Polymeric/CNT membranes

Hinds' group has pioneered a membrane fabrication strategy based on polymer encapsulation of CNT arrays[51]. They infiltrate MWNT arrays with a liquid polystyrene precursor that after curing produces a high-density MWNT membrane of ~7 nm pore size (Fig. 4d). As the process

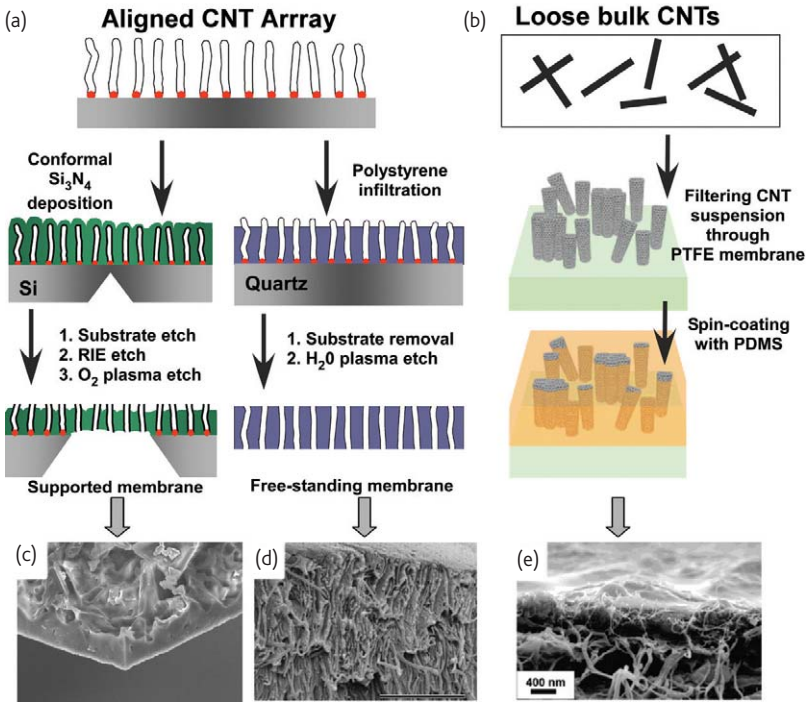

Fig. 4 Fabrication of CNT membranes. Process flow diagrams for the fabrication of CNT membranes using nanotube array encapsulation with Si_3N_4 or polymers (a), and filtration-assisted alignment (b). SEM images of a (c) Si_3N_4–encapsulated membrane, (d) polystyrene-encapsulated membrane, and (e) filtration-assisted assembly membrane. (Reproduced with permission from[53,51,54]. © 2006, 2004 American Association for the Advancement of Science and 2001 American Chemical Society, respectively.)

occurs in the liquid phase, elaborate procedures are necessary to ensure that the CNTs do not bundle together upon solvent evaporation.

Silicon nitride CNT membranes

We have developed a process for the encapsulation of a vertically aligned array of CNTs with low-stress Si_3N_x by a low pressure CVD process[52,53]. This method is widely used for a host of microfabrication processes and produces an extremely conformal coating around CNTs (Fig. 4c). The membrane produced is robust and capable of withstanding pressure gradients in excess of 1 atm. After encapsulation, the membrane undergoes a series of etching steps to remove excess Si_3N_x from the tips of the CNTs, followed by oxygen plasma to uncap the CNTs. TEM of thinned-down sections of our double-walled CNT (DWNT) membranes (Fig. 5) suggests that they consist of pores less than 2 nm in diameter, consistent with diameters of as-grown nanotubes, and no nano- or microvoids are apparent. We have demonstrated membranes with two different CNT pore diameters: DWNT with 1.1 nm < D < 2 nm and MWNT with ~6.5 nm.

CNT polymer network fabrication

A considerably different approach to producing an aligned CNT-polymer composite membrane has recently been described by Marand and coworkers (Fig. 4b)[54]. Amine-functionalized CNTs are dispersed in tetrahydrofuran and then filtered through a hydrophobic (0.2 μm) polytetrafluoroethylene (PTFE) filter, which aligns the membrane pores (Fig. 4e). Spin coating with a dilute polymer solution (polysulfone) produces a mechanically stable thin-film structure with CNT tips protruding from the top of the membrane. Membranes produced in this way exhibit enhancements in gas transport rates and non-Knudsen selectivities for binary gas mixtures. This approach has the advantage of being potentially more scalable and economical than direct CVD growth of CNTs on a substrate, although at the current stage of development the nanotube density (and thus the available pore density) is much smaller than for the membranes produced by CNT array encapsulation.

Gas transport measurements

We have measured the bulk flow rate of air through a Si_3N_4/DWNT membrane by mounting it in an O-ring sealed flow cell and applying a pressure gradient of ~1 atm[53]. To compare experimental data with simulations, we need to calculate the flow rate per nanotube and, therefore, we have to estimate the density of open pores. This estimate introduces the single largest uncertainty in the measurement of flow per pore. Plan-view TEM images of the membrane (Figs. 5c–e) allow us to estimate an upper limit to the membrane pore density (this number provides an upper limit because not all of the imaged pores span the entire 2–4 μm thickness of the membrane). This pore density estimate from TEM of 2.5×10^{11} cm^{-2} agrees well with the density of nanoparticles that catalyze nanotube synthesis. Using this number as an upper boundary, we can estimate a lower limit to the measured flow *per nanotube*. Even using this lower limit, it is readily apparent that there is a significant transport enhancement; the measured gas flows are up to 100 times greater than the predictions of the conventional Knudsen model for gas transport in rarefied environments

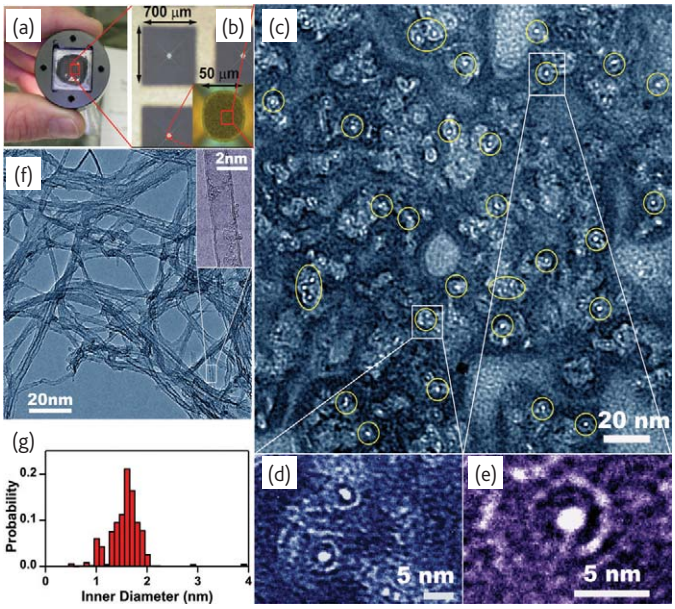

Fig. 5 Sub-2-nm CNT membranes. (a) Photograph of a CNT membrane chip in the sample holder. (b,c) Optical micrographs of the regions of the chip containing the CNT membrane windows. (c–e) High-resolution (HR) TEM images of the cross sections of the membrane showing sub-2-nm pores. HRTEM characterization of the CNT size: (f) image of dispersed CNTs from the vertically aligned array used for membrane fabrication; (g) histogram of the measured inner diameters of CNTs. (Reproduced with permission from[53]. © 2006 American Association for the Advancement of Science.)

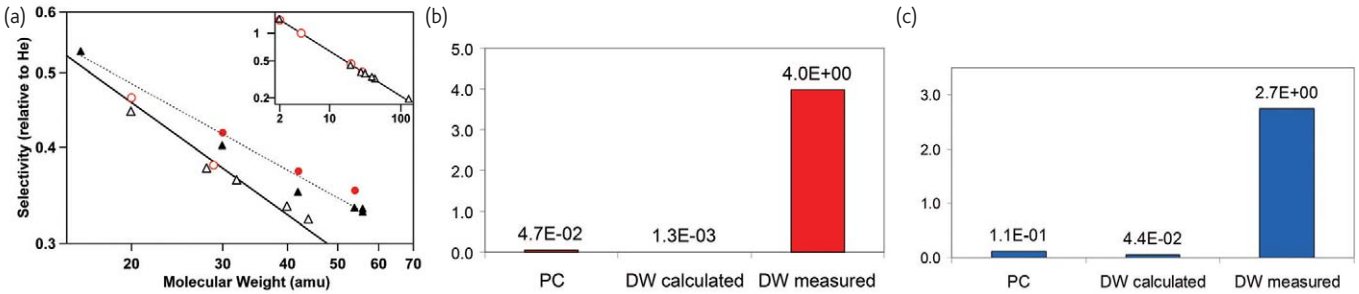

Fig. 6 Water and gas transport in sub-2-nm CNT membranes. (a) Gas selectivity (defined as the permeability relative to He) data for sub-2-nm CNT (triangles) and MWNT (circles) membranes. Open symbols denote nonhydrocarbon gases, filled symbols hydrocarbon gases. The solid line is a power law fit of the nonhydrocarbon gas selectivity data showing a scaling predicted by the Knudsen diffusion model (exponent of –0.49 ± 0.01). The dashed line is a power law fit of the hydrocarbon gas data showing a deviation from the Knudsen model (exponent of –0.37 ± 0.02). The inset shows the full mass range of nonhydrocarbon gas data, illustrating agreement with the Knudsen model scaling. (Reproduced with permission from[53]. © 2006 American Association for the Advancement of Science.) (b) Comparison of the water flux predicted for a polycarbonate (PC) membrane (left) and a DWNT (center) membrane with the flux measured for the DWNT membrane. (c) Comparison of the air flux predicted for a PC membrane (left) and a DWNT membrane (center) with the flux measured for the DWNT membrane (right).

(Fig. 6c). These experiments cannot definitively determine the cause of the observed gas flow enhancement. However, a change in the nature of molecule-wall collisions from diffuse to specular, as indicated by the MD simulations, provides a very likely explanation[42]. This conclusion is supported by the observation that nonhydrocarbon gas species tested in these experiments exhibit Knudsen-like $M^{-½}$ scaling of their membrane permeability (Fig. 6a), where M is the molecular weight.

Another interesting observation is that the sub-2-nm CNT membranes exhibit some gas selectivity for hydrocarbon transport[53]. Hydrocarbon gases show a deviation from Knudsen scaling and instead exhibit slightly higher permeabilities (Fig. 6a). This deviation in scaling may reflect additional surface adsorption and diffusion of these molecules along the surface, although more detailed measurements are needed to establish this as a viable enhancement mechanism.

Water transport in DW/MWNT membranes

We have also observed high rates of water transport through sub-2-nm DWNT membranes using pressure-driven flow[53]. Similarly high rates have also been observed by Majumder *et al.*[55] using MWNT membranes with larger pore diameters. As previously discussed, the single largest uncertainty in quantifying the flux through individual pores lies in determination of the active pore density. Majumder *et al.* estimate the active pore densities by quantifying the diffusion of small molecules through CNTs. They report enhancements of 4–5 orders of magnitude compared with the Hagen–Poiseuille formalism. As described above, we estimate the upper bounds of the pore densities so our measurements represent lower boundary estimates. The transport rates we measure reveal a flow enhancement that is at least 2–3 orders of magnitude faster than no-slip, hydrodynamic flow calculated using the Hagen–Poiseuille equation (Fig. 6b). The calculated slip length for sub-2-nm CNTs is as large as hundreds of nanometers, which is almost three orders of magnitude larger than the pore size and is almost on the order of the overall nanotube length. In contrast, a polycarbonate membrane with a pore size of 15 nm has a slip length of just 5 nm! This suggests that slip flow formalism may not be applicable to water flow through CNTs, possibly because of length scale confinement[55,56] or partial wetting between the water and the CNT surface[57].

Interestingly, the measured water flux compares well with that predicted by MD simulations[30]. The simulations predict a flux of 12 water molecules per nm^2 per ns; our measured flux, extrapolated to the simulation pressure drop, corresponds to 10–40 water molecules per nm^2 per ns[53]. Moreover, the measured absolute flow rates of at least 0.9 water molecules per nanotube is similar to the rate of 3.9 molecules/pore measured for aquaporins.

The comparison to the aquaporins is not straightforward since the diameters of our CNTs are twice that of aquaporins and are considerably longer, to name just a few differences. Therefore, we cannot yet imply that the same mechanism is responsible for transport in our CNTs and aquaporins. Nevertheless, our experiments demonstrate that water transport through CNTs starts to approach the efficiency of biological channels.

Nanofiltration properties of CNT membranes

The nearly frictionless graphitic walls of CNT composite membranes offer the unique combination of extremely fast flow and very small pore size, which potentially gives them a tremendous advantage over traditional membrane materials for energy-efficient, low-cost ultrafiltration and nanofiltration applications. Several experimental studies have used concentration-gradient or pressure-driven flow to determine the size exclusion properties of CNT composite membranes. Diffusion studies by Hinds[51,55] show that 10 nm Au nanoparticles are completely excluded by a MWNT membrane with a pore inner diameter of ~7 nm, whereas small dyes (0.5–2 nm) diffuse with low hindrance. Our aligned DWNT array membranes completely exclude 2 nm and 5 nm Au nanoparticles in pressure-driven filtration experiments. Note that at the same time the membrane exhibits very fast water permeation[53]. Ruthenium bipyridine ions, $Ru(bpy)_3^{2+}$, (1.1 nm diameter species) also permeate freely through the membrane indicating that the CNT

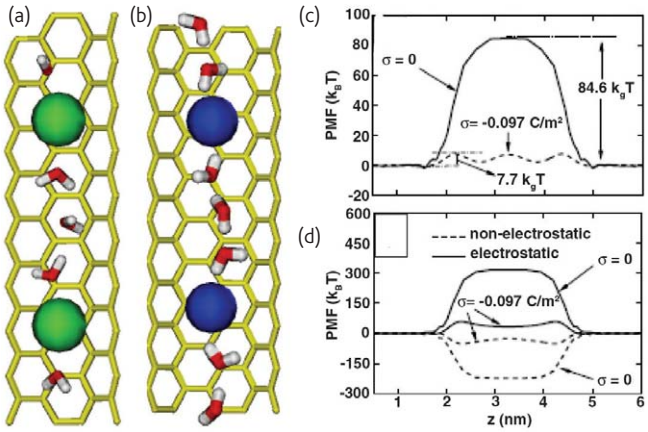

Fig. 7 MD simulations of the ion transport in CNTs. (a) Snapshot of water molecules and K^+ ions in a negatively charged (5,5) CNT. (b) Snapshot of water molecules and Cl^- ions in a positively charged (6,6) nanotube. Comparison of potential of mean force (PMF) profiles for a K^+ ion in a neutral ($\sigma = 0$) and negatively charged ($\sigma = -0.097$ C/m^2) (5,5) CNT: (c) total PFM barrier and (d) nonelectrostatic and electrostatic components of PMF. (Reproduced with from[59]. © 2006 Institute of Physics.)

diameter is in the range 1.3–2.0 nm, in excellent agreement with TEM measurements of as-grown DWNTs (Figs. 5f,g).

MD simulations of ion exclusion

With nanoscale diameters and high water permeabilities, CNTs are a promising platform for ion removal from water for desalination and demineralization. MD simulations[58,59] predict that if a nanotube is uncharged, size-based exclusion of small ionic species such as Na^+, K^+, or Cl^- requires CNT diameters of ~0.4 nm, which is comparable to the hydrated ion size. At this scale, the ion is forced to loose part of its hydration shell to enter the CNT, implying a very high energy barrier to cross the membrane (~120 kJ/mole). For slightly larger pore sizes (>1 nm), this free energy penalty decays almost to zero (~5 kJ/mole), allowing free access to small ions (Fig. 7). Molecular simulations[59] also predict that 0.34 nm diameter CNTs, decorated with negative charges along the walls, conduct K^+ ions while excluding Cl^-, whereas positively charged 0.47 nm diameter CNTs exclude K^+ ions while conducting Cl^-. Experimental verification of these predictions has not yet been achieved as CNT membranes with such small pore openings have not been fabricated to date. Joseph *et al.*[60] have shown that the presence of charged groups on open CNT tips induces preferential ion transport for CNT diameters of 2.2 nm. These results in particular suggest that dedicated functionalization of small-diameter CNT membranes (such as those demonstrated by Holt *et al.*[53]) may enable the control of ionic flow or even the exclusion of very small ions, an exciting prospect for water purification and desalination.

Membrane functionalization and transport

An important avenue for controlling transport through nanotube channels involves using chemical modifications of the nanotube to alter the channel permeability or size exclusion characteristics, or even construct an controllable 'gate' to regulate the transport efficiency based on an external stimulus. To maintain efficient flow through a nanotube, these treatments have to preserve the fundamental smoothness and hydrophobicity of the nanotube walls. Therefore, we will concentrate on modification strategies that target only the entrance and exit of the nanotube. In fact, most membrane fabrication strategies facilitate this approach by using an oxidation step to remove the fullerene cap from the nanotube. This typically produces carboxylic groups at the mouth of the nanotube[61], which can then serve as the target for a variety of chemical modification approaches[62,63].

Most recent progress in this area has been associated with the work of Hinds and coworkers who have used carbodiimide chemistry to attach a variety of organic and biological molecules to the mouth of CNTs. Interestingly, they observe that, for polymer-matrix-based aligned nanotube membranes, the idealized picture of the oxidation step producing only a ring of carboxylic acid groups on the nanotube end and leaving the rest of the nanotube intact misrepresents reality. Experiments on decorating nanotube surfaces with Au nanoparticles show that oxidation produces reactive groups in regions of the nanotube up to 700 nm away from the tip[63,64], although after only 50 nm of separation from the tip the functional group density is significantly reduced. The researchers argue[63] that these apparently large penetration depths are consistent with observations that the process produces exposed CNT tips above the polystyrene matrix.

Majumder *et al.*[63] have used carbodiimide chemistry to attach aliphatic chains, charged dye molecules, and polypeptides to polystyrene-based CNT membranes. These modifications have a measurable effect on the flux of the two large organic cations (methyl viologen (Mv^{2+}), and $Ru(bpy)_3^{2+}$) used: for example, attaching a C_{40} alkane chain reduces the flux of Mv^{2+} by six times. Interestingly, they do not observe a clear trend in the effect of the modification on the flux of the test species: for example, attaching a bulky charged organic dye to the mouth of the CNT membrane actually increases the ion flux, presumably because of interactions of the dye molecules with the oppositely charged ions[63]. The effect of the size of the modifier group on the charged species flux is also complex; the researchers speculate that longer hydrophobic aliphatic chains prefer to orient along CNT walls and thus have a reduced effect on the overall flux.

Recently, Majumder *et al.*[65] have used charged organic dye molecules to regulate transport through CNT membranes as a function of an external applied voltage. Ideally, the function of such a system would be analogous to the operation of voltage-gated ion channels. The work uses an innovative modification procedure whereby a constant flow of an inert solution through the nanotube membrane helps to protect the inner walls of the nanotube and localizes the modification to the rim of the nanotube. After modification, there is evidence that the applied voltage can draw the grafted charged dye molecules from the pore entrance into the nanotube core.

Unfortunately, the observed response of the modified membrane to the voltage gating is complex, with both positive and negative voltages modulating the membrane flux. This complexity is likely to be a result of using charged ion species as transport reporters. Further studies should provide a more detailed picture of the interaction in this system.

Outlook: CNT membranes as a scientific and technological platform

The nanoscale size and atomically smooth surfaces of CNTs offer a unique system for studying molecular transport and nanofluidics. In particular, an understanding of the behavior of water and ions in confined geometries is crucial for many biological and geological processes. In the past 5–10 years, it has become possible to perform MD simulations on relatively large systems over longer time periods. These advances have enabled the simulation of molecules inside CNTs and have predicted several counterintuitive phenomena. More recently, the development of experimental platforms that allow the study of molecular confinement inside CNTs is starting to validate the predictions of simulations. Although there is still no real consensus in the understanding of the effects of confinement, we are confident that a coherent picture of these phenomena will soon emerge.

Understanding the fundamentals, namely the transport mechanisms and molecular structure within CNTs, will allow us to exploit the high permeabilities characteristic of CNTs and develop membrane-based transformational technologies for separation and purification. The fast flow and small pore size of CNT membranes promise considerable energy reductions in desalination and gas separations. The use of CNT as fluidic channels also opens up an opportunity for true molecular-scale transport gating, since the size of the pore is comparable to the size of large organic molecules and has important implications for the development of protective gear and drug delivery systems.

Acknowledgments

CPG and OB acknowledge support from NSF NER 0608964; AN, CPG, and OB NSF NIRT CBET-0709090. Parts of this work were performed under the auspices of the US Department of Energy by the University of California, Lawrence Livermore National Laboratory under Contract W-7405-Eng-48.

REFERENCES

1. Batchelor, G. K., ***An Introduction to Fluid Dynamics***, Cambridge University Press, (1967)
2. Travis, K. P., *et al.*, *Phys. Rev. E* (1997) **55**, 4288
3. Qiao, R., and Aluru, N. R., *J. Chem. Phys.* (2003) **118**, 4692
4. Huang, C. K., *et al.*, *J. Chem. Phys.* (2007) **126**, 224702
5. Terrones, M., *Annu. Rev. Mater. Res.* (2003) **33**, 419
6. Dresselhaus, M. S., *et al.*, *Physical Properties of CNTs*, Imperial College Press (1998)
7. Yamada, T., *et al.*, *Nat. Nanotechnol.* (2006) **1**, 131
8. Futaba, D. N., *et al.*, *Nat. Mater.* (2006) **5**, 987
9. Cheung, C. L., *et al.*, *J. Phys. Chem. B* (2002) **106**, 2429
10. Loiseau, A., *et al.*, Synthesis Methods and Growth Mechanics. In: *Understanding Carbon Nanotubes*, Lecture Notes in Physics Series, Springer ,(2006) **677**, 49
11. Franklin, N. R., *et al.*, *Appl. Phys. Lett.* (2002) **81**, 913
12. Puretzky, A. A., *et al.*, *Appl. Phys. A* (2005) **81**, 223
13. Hummer, G., *Mol. Phys.* (2007) **105**, 201
14. Hummer, G., *et al.*, *Nature* (2001) **414**, 188
15. Kolesnikov, A. I., *et al.*, *Phys. Rev. Lett.* (2004) **93**, 35503
16. Naguib, N., *et al.*, *Nano Lett.* (2004) **4**, 2237
17. Maniwa, Y., *et al.*, *Nat. Mater.* (2007) **6**, 135
18. Mamontov, E., *et al.*, *J. Chem. Phys.* (2006) **124**, 194703
19. Waghe, A., *et al.*, *J. Chem. Phys.* (2002) **117**, 10789
20. Beckstein, O., *et al.*, *J. Phys. Chem. B* (2001) **105**, 12902
21. Beckstein, O., and Sansom, M. S. P., *Proc. Natl. Acad. Sci. USA* (2003) **100**, 7063
22. Allen, R., *et al.*, *Phys. Rev. Lett.* (2002) **89**, 175502
23. Allen, R., *et al.*, *J. Chem. Phys.* (2003) **119**, 3905
24. Andreev, S., *et al.*, *J. Chem. Phys.* (2005) **123**, 194502
25. Wang, J., *et al.*, *Phys. Chem. Chem. Phys.* (2004) **6**, 829
26. Won, C. Y., *et al.*, *J. Chem. Phys.* (2006) **125**, 114701
27. Huang, L.-L., *et al.*, *Phys. Chem. Chem. Phys.* (2006) **8**, 3836
28. Mashl, R. J., *et al.*, *Nano Lett.* (2003) **3**, 589
29. Won, C. Y., and Aluru, N. R., *J. Am. Chem. Soc.* (2007) **129**, 2748
30. Kalra, A., *et al.*, *Proc. Natl. Acad. Sci. USA* (2003) **100**, 10175
31. Sui, H., *et al.*, *Nature* (2001) **414**, 872
32. Murata, K., *et al.*, *Nature* (2000) **407**, 599
33. Agre, P., *et al.*, *Curr. Top. Membranes* (2001) **51**, 1
34. Kotsalis, E. M., *et al.*, *Int. J. Multiph. Flow* (2004) **39**, 995
35. Hanasaki, I., and Nakatani, A., *J. Chem. Phys.* (2006) **124**, 144708
36. Striolo, A., *Nano Lett.* (2006) **6**, 633
37. Schlichting, I., *et al.*, *Science* (2000) **287**, 1615
38. Pomes, R., and Roux, B., *Biophys. J.* (1996) **71**, 19
39. Brewer, M. L., *et al.*, *Biophys. J.* (2001) **80**, 1691
40. Dellago, C., *et al.*, *Phys. Rev. Lett.* (2003) **90**, 105902
41. Sorin, E. J., and Pande, V. S., *J. Am. Chem. Soc.* (2006) **128**, 6316
42. Skoulidas, A. I., *et al.*, *Phys. Rev. Lett.* (2002) **89**, 185901
43. Skoulidas, A. I., *et al.*, *J. Chem. Phys.* (2006) **124**, 054708
44. Chen, H., *et al.*, *J. Phys. Chem. B* (2006) **110**, 1971
45. Chen, H. and Sholl, D. S., *J. Am. Chem. Soc.* (2004) **126**, 7778
46. Sokhan, V. P., *et al.*, *J. Chem. Phys.* (2004) **120**, 3855
47. Sokhan, V. P., *et al.*, *J. Chem. Phys.* (2001) **115**, 3878
48. Sokhan, V. P., *J. Chem. Phys.* (2002) **117**, 8531
49. Sun, L., and Crooks, R. M., *Langmuir* (1999) **15**, 738
50. Che, G., *et al.*, *Chem. Mater.* (1998) **10**, 260
51. Hinds, B. J., *et al.*, *Science* (2004) **303**, 62
52. Holt, J. K., *et al.*, *Nano Lett.* (2004) **4**, 2245
53. Holt, J. K., *et al.*, *Science* (2006) **312**, 1034
54. Kim, S., *et al.*, *Nano Lett.* (2007) **7**, 2806
55. Majumder, M., *et al.*, *Nature* (2005) **438**, 44
56. Cottin-Bizonne, C., *et al.*, *Euro. Phys. J. E* (2002) **9**, 47
57. Craig, V. S. J., *et al.*, *Phys. Rev. Lett.* (2001) **87**, 54504
58. Peter, C., and Hummer, G., *Biophys. J.* (2005) **89**, 2222
59. Park, J. H., *et al.*, *Nanotechnology* (2006) **17**, 895
60. Joseph, S., *et al.*, *Nano Lett.* (2003) **3**, 1399
61. Hiura, H., *et al.*, *Adv. Mater.* (1995) **7**, 275
62. Wong, S. S., *et al.*, *Nature* (1998) **394**, 52
63. Majumder, M., *et al.*, *J. Am. Chem. Soc.* (2005) **127**, 9062
64. Chopra, N., *et al.*, *Adv. Func. Mater.* (2005) **15**, 858
65. Majumder, M., *et al.*, *Langmuir* (2007) **23**, 8624